Soil Dynamics and Earthquake Engineering 31 (2011) 240–246

Contents lists available at ScienceDirect

Soil Dynamics and Earthquake Engineering

journal homepage: www.elsevier.com/locate/soildyn

An examination of τ_c-Pd earthquake early warning method using a strong-motion building array

Jang-Tian Shieh [a], Yih-Min Wu [a,*], Li Zhao [b], Wei-An Chao [a], Chien-Fu Wu [c]

[a] Department of Geosciences, National Taiwan University, No. 1, Sec. 4th, Roosevelt Rd, Taipei 106, Taiwan
[b] Institute of Earth Sciences, Academia Sinica, Taipei 115, Taiwan
[c] Central Weather Bureau, Taipei 100, Taiwan

ARTICLE INFO

Article history:
Received 15 August 2009
Received in revised form
2 December 2009
Accepted 21 December 2009

Keywords:
Earthquake early warning
Strong-motion record
Taitung earthquake
Taiwan

ABSTRACT

The use of characteristic period τ_c and peak displacement amplitude *Pd* of the initial P wave in earthquake early warning (EEW) was proposed by Wu and Kanamori [1–4]. Here we apply this approach to strong-motion records from a building sensor array installed in Taitung County, Taiwan. This building was damaged during the 2006 M_w=6.1 Taitung earthquake with a peak ground velocity (PGV) of up to 38.4 cm/s at an epicentral distance of 14.5 km. According to our analysis, the peak displacement amplitude *Pd* is a better indicator for the destructiveness of an earthquake than τ_c because τ_c is more sensitive to the signal-to-noise ratio (SNR) than *Pd*. In accordance with previous studies, only the structurally damaging Taitung earthquake generated a *Pd* value larger than 0.5 cm (a threshold for identifying damaging events). Using *Pd* as an indicator for destructive earthquakes does not lead to missing or false alarms for EEW purposes.

1. Introduction

Taiwan is located on the western circum-Pacific seismic belt with a measured plate boundary convergence rate of about 8 cm/year [5] and has been repeatedly hit by damaging earthquakes [6]. Some of the disastrous events have inflicted severe casualties and great property losses. In all likelihood the damages caused by earthquakes will continue and even increase as the population and the economy grow. It is therefore crucial for Taiwan to seek means for alleviating the earthquake losses through scientific research. EEW system has become one of the most effective tools for real-time seismic hazard mitigation [7]. In a well-established EEW system, the characteristic period τ_c and the peak displacement amplitude *Pd* of the initial P wave are two important parameters, and they have been used to determine the magnitudes and the shaking intensity [1–4,8–11] of earthquakes. Furthermore, the parameter *Pd* can also be used for magnitude estimation for EEW purpose [12,13]. Frequent earthquakes and abundant high-quality near-field strong-motion records in Taiwan provide valuable data for examining the efficacy of the τ_c and *Pd* methods for practical earthquake early warning purpose.

In this study, we use the strong-motion records from a building sensor array in Taitung, Taiwan, to perform the EEW analysis. The strong-motion sensors were installed in 1996 in a building belonging to the fire bureau of Taitung County, Taiwan. The building was damaged during the 2006 M_w=6.1 Taitung earthquake [14]. Fig. 1 shows photographs of this building before and after that damaging event. Before the Taitung earthquake, this system had recorded a number of small to large earthquakes, including the 1999 M_w=7.6 Chi-Chi (epicentral distance = 125.0 km and PGV = 7.1 cm/s, [15]) and the 2003 M_w=6.8 Chengkung (epicentral distance = 42.2 km and PGV = 23.5 cm/s, [16]) earthquakes. However, those relatively large events had not caused damage to this building. The valuable records from those earthquakes provided by this sensor array offer an excellent opportunity for us to examine the use of τ_c and *Pd* measurements at a single site for onsite EEW purpose. Furthermore, different placements of sensors around the building allow us to study the impact of the locations of seismometers on the results in EEW analyses.

2. Data

The strong-motion records come from sensors distributed in the building with 4 floors above ground and one in the basement. Force balance acceleration (FBA) sensors were deployed at specific locations on each floor, and an additional one with three free-field channels was installed outside of the building. The network is comprised of a total of 22 channels with a central recording system on a personal computer. Among the channels 6 are vertical

* Corresponding author. Tel.: +886 2 2362 0054; fax: +886 2 23644625.
E-mail address: drymwu@ntu.edu.tw (Y.-M. Wu).

0267-7261/$ - see front matter © 2009 Elsevier Ltd. All rights reserved.
doi:10.1016/j.soildyn.2009.12.015

components, and the others are horizontal ones. The channels are distributed as follows: 3 in the basement, 5 on the 1st floor, 4 on the 2nd floor, 7 at roof level, and the 3 free-field channels near the back door of the building. Fig. 2 shows the distribution of all the sensors installed in the building.

Fig. 1. Photos showing the building under study before and after the destructive 2006 M_w=6.1 earthquake.

Between 1996 and 2006, there were 88 earthquakes recorded by this system. Table 1 lists the 69 events selected for analysis in this study. The selection was based on two criteria. First, our method requires at least one vertical and two orthogonal horizontal channels in each location. Second, some events were either not triggered by the automatic P arrival picking procedure [17] or having instrumental problems. Fig. 3 shows the distribution of the epicenters of selected events and the location of the building under study.

We use the local magnitude M_L [18,19] in our analysis. For events with M_L larger than 6, however, we replace the magnitude values by their moment magnitude, M_w, in consideration of the saturation problem of M_L. Both types of magnitudes are simply denoted by M in this study.

3. Analysis

The original acceleration records were integrated twice to obtain the displacements. Following the practice in our previous studies [1–4], a two-pole Butterworth high-pass filter with a corner frequency of 0.075 Hz was applied to the displacements in order to remove the long period drift, and the filtered displacements were then differentiated to obtain the velocity waveforms. The peak acceleration amplitude Pa, peak velocity amplitude Pv, and the peak displacement amplitude Pd are determined from the vertical components of the acceleration and the filtered velocity and displacement waveforms within the 3-s window after the P arrival. The characteristic period of the initial P wave, τ_c, is also determined from the 3-s vertical-component waveform after the P arrival in the same manner as discussed in previous studies. Fig. 4 provides an example showing the original accelerogram, filtered velocity and filtered displacement waveforms along with the measured Pa, Pv, and Pd. Also shown for the same example are the peak amplitudes of the total acceleration (A^{max}) and filtered velocity (V^{max}) and displacement (D^{max}) in the building array record. In this study, the peak amplitudes A^{max}, V^{max}, and D^{max} are

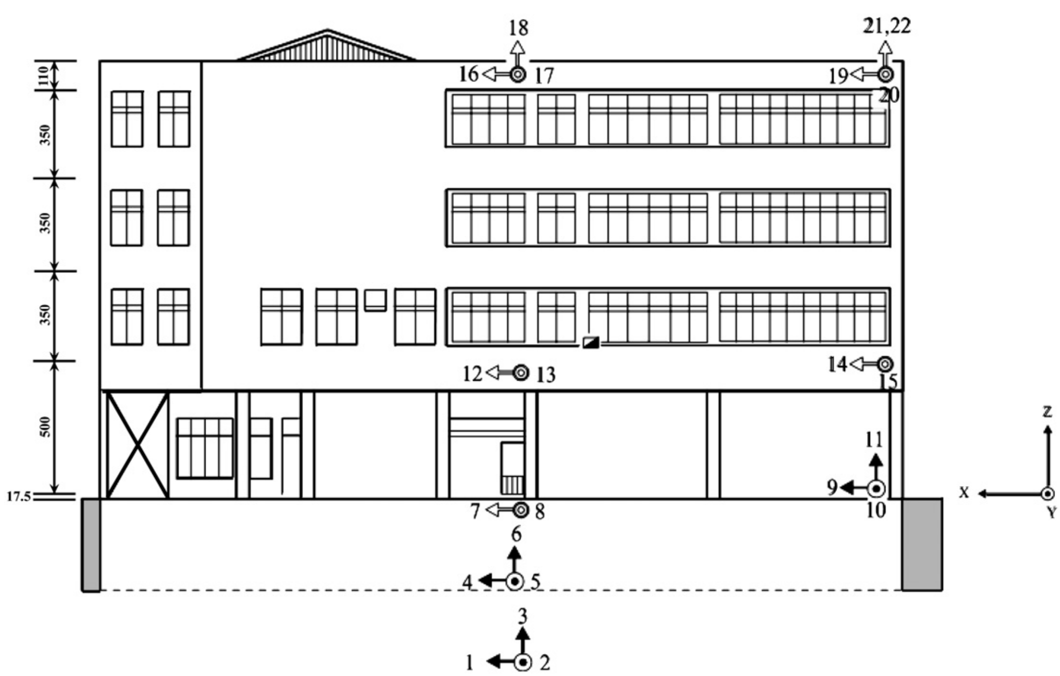

Fig. 2. Distribution of strong motion sensors installed in the building.

Table 1
Parameters of 69 events selected and analyzed in this study.

Origin time (UT)	Longitude (E)	Latitude (N)	Depth (km)	Distance[a] (km)	M	PGA (gal)	PGV (cm/s)	PGD (cm)
1996/09/05 23:42	121.367	22.001	14.8	87.7	6.8	14.08	2.04	0.82
1996/12/18 02:50	121.378	22.803	16.3	24.3	4.9	12.04	0.36	0.08
1996/12/18 11:20	121.358	22.821	16.2	22.7	5.0	7.79	0.52	0.10
1997/01/29 06:43	121.098	22.803	18.5	6.3	4.3	21.68	1.20	0.08
1997/03/24 10:26	121.378	22.729	11.1	24.3	4.5	5.06	0.19	0.06
1997/05/03 02:46	121.402	22.537	3.6	36.6	5.3	7.32	0.71	0.17
1997/06/07 02:02	121.072	22.605	19.8	19.3	4.2	10.17	0.33	0.09
1997/10/17 13:14	121.43	22.817	25.6	29.8	4.7	4.96	0.24	0.10
1997/10/22 11:16	121.463	22.444	10.2	48.4	5.3	4.35	0.33	0.14
1998/01/18 19:56	121.089	22.725	3.3	7.3	5.1	64.71	2.07	0.33
1998/01/20 23:29	121.08	22.686	3.8	11.1	5.1	23.49	1.02	0.12
1998/01/21 03:30	121.067	22.722	10.4	9.4	4.1	14.78	0.39	0.04
1998/06/22 22:47	121.019	22.574	14.5	24.9	4.1	3.20	0.09	0.12
1998/07/17 04:51	120.662	23.503	2.8	95.4	5.7	4.74	0.74	0.56
1998/11/17 22:27	120.790	22.832	16.5	37.2	5.5	9.24	0.88	0.20
1999/08/04 21:03	121.142	22.789	16.4	2.6	4.81	21.81	1.28	0.12
1999/09/04 12:54	121.116	22.812	21.3	5.9	4.4	14.38	0.43	0.09
1999/09/20 17:47	120.815	23.853	8.0	125.0	7.6	21.50	7.06	6.79
1999/09/20 18:11	121.070	23.860	12.5	122.0	6.7	7.56	1.92	0.87
1999/09/20 21:46	120.857	23.585	8.6	95.4	6.4	11.55	3.42	3.58
1999/09/22 00:14	121.047	23.826	15.6	117.8	6.4	17.40	2.96	0.98
1999/09/25 20:51	121.004	23.130	7.3	42.8	5.0	8.02	0.41	0.14
1999/09/25 23:52	121.002	23.854	12.1	121.4	6.5	10.58	1.99	1.05
1999/10/22 02:18	120.423	23.517	16.6	111.3	5.8	5.11	0.56	0.25
1999/10/22 03:10	120.431	23.533	16.7	112.1	5.5	6.10	0.80	0.26
1999/11/01 17:53	121.726	23.362	31.3	88.9	6.3	8.91	1.21	0.56
2000/02/03 18:48	121.262	22.787	18.3	12.2	4.9	21.11	0.87	0.17
2000/02/03 18:57	121.251	22.850	8.6	14.3	4.2	6.07	0.23	0.12
2000/02/15 21:33	120.740	23.316	14.7	73.7	5.6	5.96	0.46	0.10
2000/02/22 15:42	121.152	22.499	24.5	29.6	4.8	5.00	0.18	0.14
2000/05/17 18:12	121.308	22.842	25.1	18.7	4.7	4.62	0.20	0.17
2000/08/20 10:51	120.842	23.097	9.0	48.1	4.5	10.46	0.47	0.09
2000/08/21 16:42	120.958	22.947	4.1	27.7	4.8	4.70	0.16	0.07
2001/03/23 01:03	121.339	22.774	29.8	19.9	4.5	11.36	0.26	0.19
2001/12/27 08:34	121.096	22.716	12.9	7.5	4.8	45.41	2.17	0.33
2002/01/07 02:45	120.898	22.976	7.7	34.4	4.8	4.61	0.22	0.07
2002/04/20 08:48	121.630	22.826	19.9	50.2	5.1	9.70	0.79	0.15
2002/04/28 04:37	121.354	22.889	20.5	25.4	4.3	6.26	0.42	0.12
2002/05/30 17:27	121.418	22.787	16.3	28.1	4.7	7.16	0.24	0.11
2002/09/24 22:43	121.076	22.669	9.7	12.9	5.2	44.32	3.24	0.55
2003/06/10 08:40	121.699	23.504	32.3	99.5	5.9	14.06	1.20	0.28
2003/09/10 22:55	121.399	22.709	85.7	26.8	5.8	5.31	0.33	0.08
2003/12/10 04:38	121.398	23.067	17.7	42.2	6.8	143.05	23.47	8.10
2003/12/10 05:20	121.221	23.075	3.4	35.1	5.2	16.19	1.44	0.36
2003/12/10 08:35	121.368	22.837	18.6	24.2	4.4	4.54	0.12	0.12
2003/12/10 08:46	121.363	22.87	26.4	25.2	5.2	16.96	0.92	0.21
2003/12/11 00:01	121.392	22.792	33.6	25.5	5.4	31.28	1.31	0.43
2003/12/11 19:04	121.294	22.941	22.1	24.7	4.7	4.77	0.21	0.16
2003/12/11 22:57	121.192	23.051	7.0	31.9	4.7	3.83	0.34	0.19
2003/12/17 16:27	121.311	22.606	32.2	24.6	5.4	9.38	0.77	0.32
2003/12/18 05:33	121.082	22.842	12.5	10.6	5.0	36.52	2.94	0.25
2003/12/18 16:16	121.069	22.861	9.6	13.1	4.2	14.07	0.65	0.23
2004/01/05 11:07	121.300	22.860	19.0	19	4.8	10.68	0.45	0.22
2004/01/28 19:13	120.952	22.992	6.7	31.9	5.2	20.45	0.95	0.12
2004/01/28 19:34	120.925	23.006	2.5	34.9	5.0	9.44	0.36	0.10
2004/03/13 05:03	121.412	22.984	35.4	36.5	5.0	4.51	0.18	0.17
2004/06/10 15:58	121.015	22.898	13.7	19.8	4.9	17.16	0.73	0.16
2004/08/14 03:29	120.980	22.930	1.1	24.8	4.3	15.09	0.50	0.10
2004/10/16 14:36	121.082	22.793	12.3	7.1	4.1	9.58	0.36	0.04
2005/01/08 03:27	120.988	22.953	8.3	26.2	4.1	6.77	0.27	0.09
2005/01/22 06:54	121.270	22.880	18.9	18.3	4.3	5.95	0.18	0.12
2005/02/18 20:18	121.674	23.34	15.3	83.5	5.6	2.57	0.25	0.20
2005/05/08 18:54	121.083	22.878	13.5	13.9	4.1	3.65	0.16	0.06
2005/07/07 05:07	121.086	22.872	13.6	13.2	4.2	4.10	0.17	0.09
2005/12/28 22:17	121.15	22.937	20.5	18.9	4.8	5.01	0.19	0.10
2006/04/01 10:02	121.081	22.883	7.2	14.5	6.1	385.65	38.39	5.3
2006/04/01 10:05	121.076	22.900	8.7	16.4	4.6	12.25	0.75	0.48
2006/04/01 10:40	121.111	22.859	11.5	10.9	4.8	6.73	0.40	0.28
2006/04/04 12:49	121.098	22.875	9.9	13.0	4.5	5.30	0.19	0.11

[a] Distance from the epicenter to the study site.

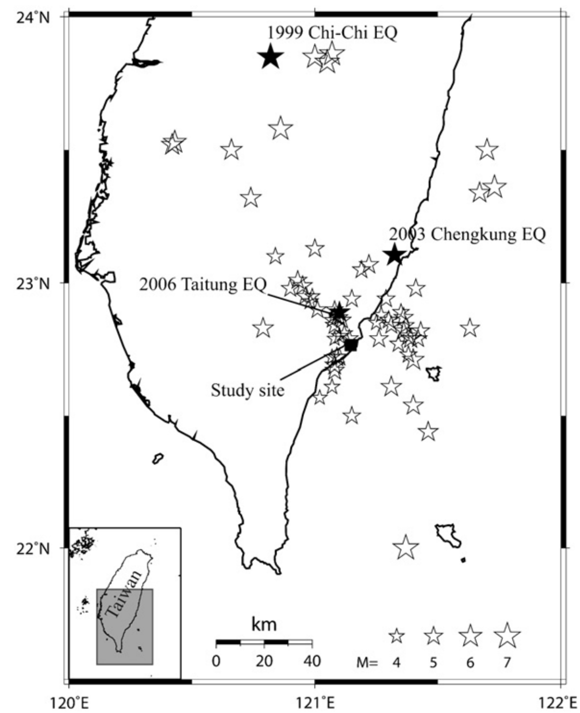

Fig. 3. Solid square shows the location of the building under study. Epicenters of events recorded by this building array system from 1996 to 2006 are marked by stars with sizes representing the earthquake magnitudes. Solid stars indicate the epicenters of the 2006 Taitung M_w=6.1, the 2003 Chengkung M_w=6.8, and the 1999 Chi-Chi M_w=7.6 earthquakes.

obtained from the three components of the records in the building. The peak ground velocity (PGV) is obtained from the three components of the waveform recorded on the free-field site.

Generally speaking, the τ_c values measured from various stations must be averaged to reduce the scattering due to site or source effects. In this study, we average the τ_c values obtained from different kinds of positions in the building. Results show that for events with lower magnitudes, the τ_c values tend to have larger scattering, and many of them are unreasonably large (Fig. 5A). Even after removing values above 10 s that are considered unreasonable for the high pass filter with a 0.075-Hz corner frequency, the scattering is still too large.

With regards to the effectiveness in the EEW system, the relation of *Pa*, *Pv*, and *Pd* versus the PGV, generally considered as an indicator of the destructiveness of earthquakes, was compared. In this study, the PGV is measured from the free-field channels. We found that there is a much clearer gap in the *Pd* values between the Taitung earthquake and other non-destructive ones than in the *Pa* or *Pv* values, as suggested in previously study [2]. The *Pd* versus PGV distribution in Fig. 6 shows that except for the destructive Taitung event, no *Pd* value of any other record exceeds 0.5 cm. This confirms the result of Wu and Kanamori [2,4] that led them to advocate the use of 0.5 cm in the *Pd* value as an indicator of a destructive earthquake.

Relationships of *Pd* versus the free-field PGV and the V^{max} values from 3 channels at a location on the roof floor (Channels 19, 20, and 21 shown in Fig. 2) are compared in Fig. 7. Measurements from the roof floor show a better linear fit. Measurements at both sites yield small linear correlation coefficient values (R), which may be due to the limited number of records. Nevertheless, similar slopes are obtained from the

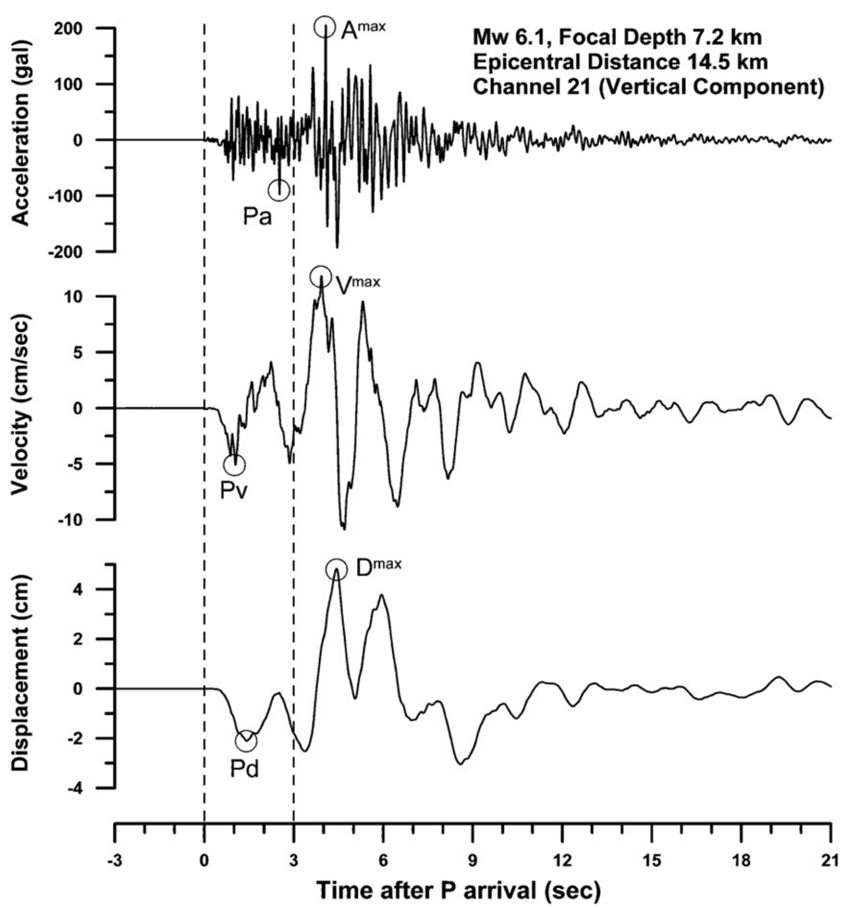

Fig. 4. An example showing the *Pa*, *Pv*, *Pd*, A^{max}, V^{max}, and D^{max} measurements marked by open circles. The two dashed lines show the 3-second time window after the P arrival.

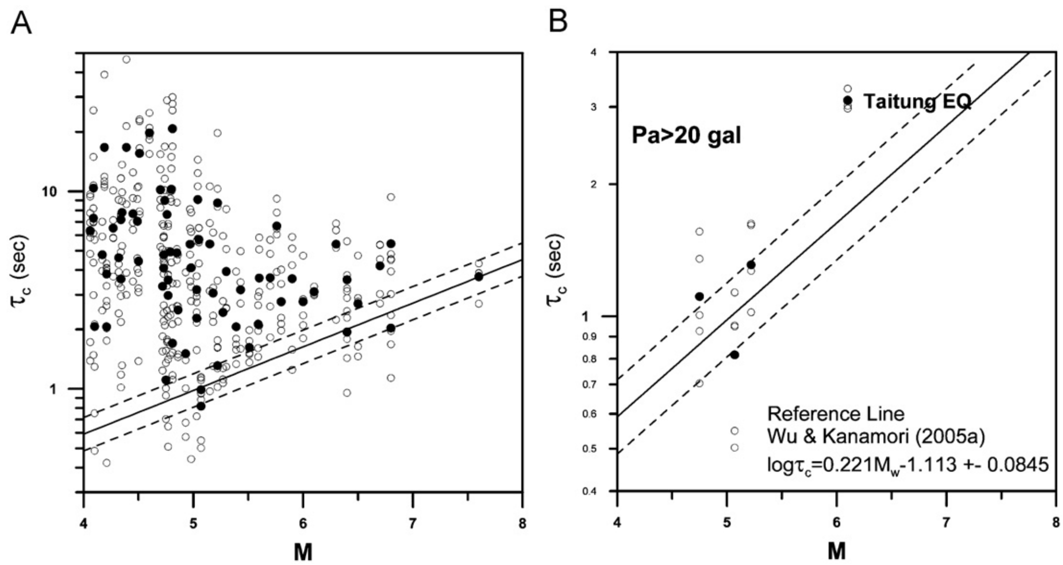

Fig. 5. Initial P-wave characteristic period τ_c determined from vertical-component records. Open circles represent τ_c of each record and solid circles represent the averaged τ_c values from records of the same event. (A) For all vertical-component records. (B) For records with average *Pa*>20 gal. In each plot the solid line shows the best fit line determined by Wu and Kanamori [1] and the two dashed lines show the range of one-standard deviation.

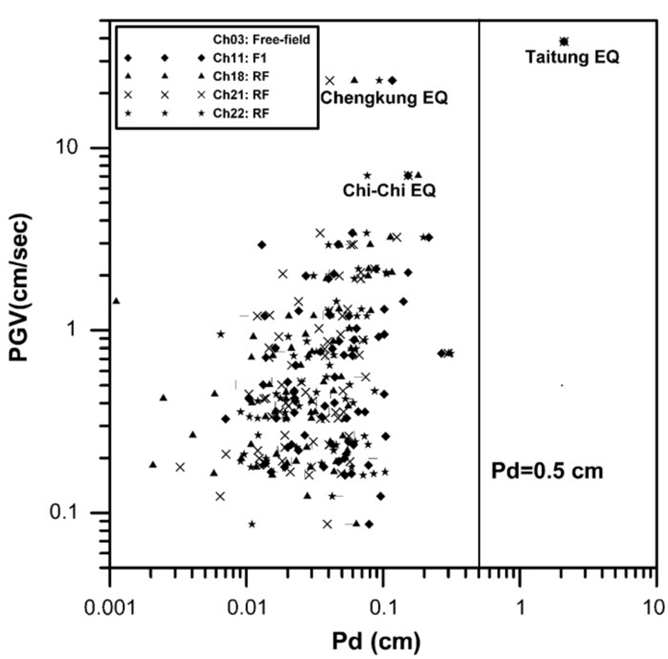

Fig. 6. Initial P-wave peak displacement amplitude *Pd* measurements of the study building versus PGV measured from free-field.

linear fits to the measurements at both sites. This observation highlights the fact that the building only amplifies the signals on the higher floors, but it does not change the scaling relation between *Pd* and *PGV* or V^{max}. Thus, it may not be necessary to install seismometers inside this building for the EEW purpose. A sensor at a free-field site is perhaps sufficient.

4. Discussion

In this study, we found that the correlation between the initial P-wave characteristic period τ_c and magnitude is not as good as in previous studies [10,11]. One of the reasons for the scattering in the data may be the low signal-to-noise ratio (SNR) of the strong-motion waveforms recorded by the FBA sensors with a 16-bit resolution and a full scale of ± 2 g. The scattering can be reduced when records with *Pa* values less than 20 gal are removed (Fig. 5B). However, the results of Wu et al. [10] using earthquakes in Southern California show a clear scaling between τ_c and magnitude when they removed the measurements with *Pa* values less than 2.5 gal. The discrepancy between the two studies may be a result of the difference in equipment. In Wu et al. [10], most of the stations used are equipped with both high-gain broad-band velocity and low-gain FBA sensors with signals digitized at 100 or 80 samples per second with a 24-bit resolution. In comparison to the strong-motion building array used in this study, the combination of broad-band and strong-motion sensors in earthquake monitoring can provide signals with higher SNR and still record large events with large dynamic range. In a separate study by Shieh et al. [11] using the Japanese K-net strong-motion array records with a sampling rate of 100 Hz at a 24-bit resolution and a full scale of ± 2 g, a good scaling was observed between magnitude and τ_c. Even though the strong-motion sensors record signals with lower SNR than broad-band sensors, the combination of the 24-bit resolution and their data selection of only 6 nearest records from each event with M_w equal to or larger than 6 provides a good SNR for their analysis. Results from these three studies indicate that τ_c may be too sensitive to the SNR, as indicated by Wu et al. [10].

In Fig. 5B, the destructive Taitung earthquake shows a much larger τ_c, far from the best-fit line determined in previous studies [1–4]. This may be explained by the near-source effect proposed by Yamada and Mori [20]. They argued that when *Pd* exceeds 1 cm and τ_c exceeds 2 s, τ_c is likely to be overestimated because of the near-field effect. The fact that Taitung earthquake with M_w=6.1 has a *Pd* value of up to 2.16 cm and a τ_c of up to 3.3 s may be one of the reasons.

It is notable that the 2003 M_w=6.8 Chengkung earthquake has a significantly larger PGV corresponding to its *Pd* value (Fig. 7). This could be explained by either source or path effect. Huang et al. [21] suggested that the fault rupture propagated from the north end southward and the study site is in the southwest of the epicenter. Ground-motion amplitude at the study site may

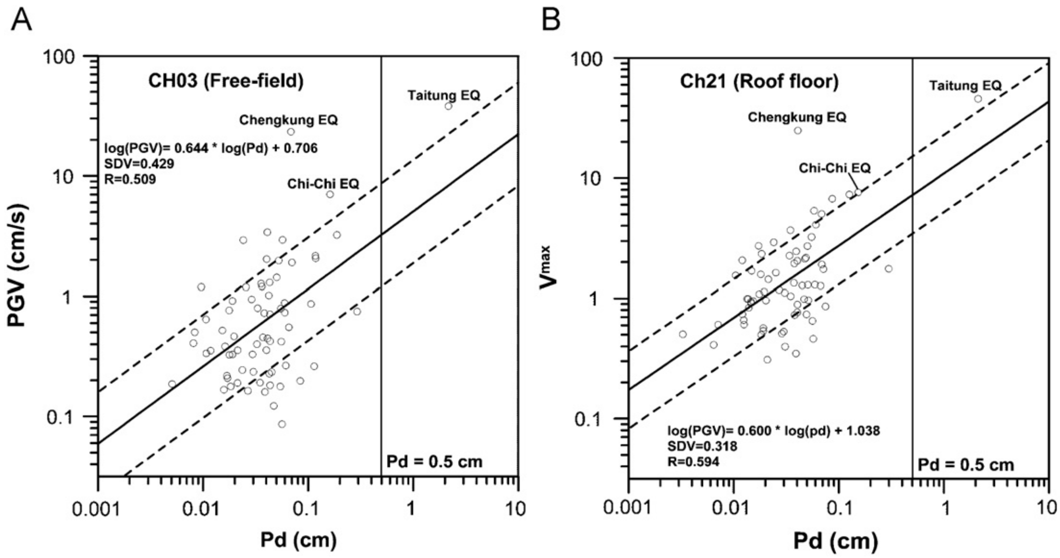

Fig. 7. (A) PGV at free-field. (B) V^{max} at a specific location on the roof floor versus *Pd*. The solid line and two dashed lines in each plot show the best fit line and the range of one-standard deviation, respectively.

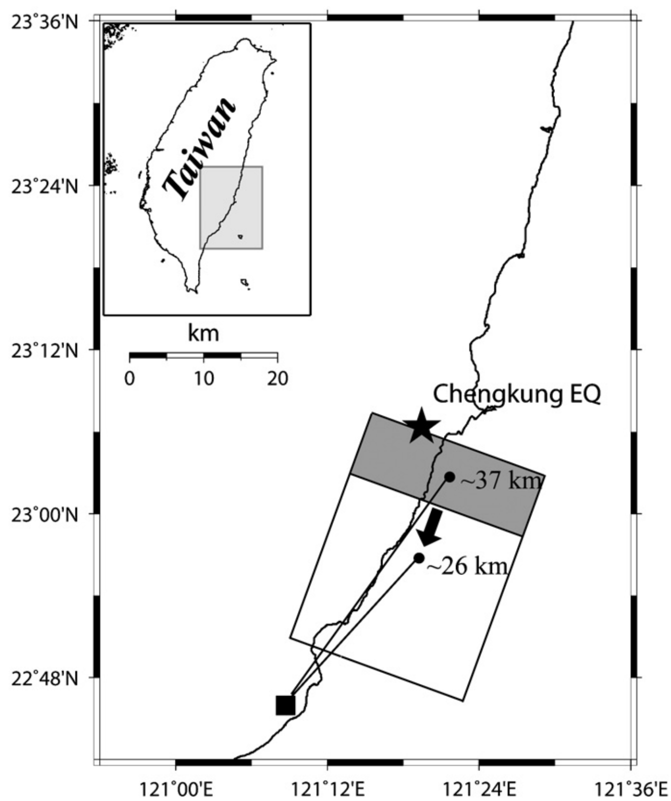

Fig. 8. Fault model of the Chengkung earthquake proposed by Wu et al. [14]. Grey area shows the first 3-s rupture region.

be amplified by the directivity effect. While PGV can be affected by the total rupture process, *Pd*, measured from the first 3 s after the P wave, may only be influenced by the initial rupture. Fig. 8 shows the fault model determined by Wu et al. [16]. Assuming a rupture velocity of 3 km/s, the rupture in the first 3 s covered about 10 km in the north portion of the fault. It can be observed that the ray paths from the first 3 s of the rupture to the site are longer than those of the later rupture. In considering the seismic wave attenuation, *Pd* may not have the same scaling relation as PGV.

5. Summary

In this study, we found that τ_c do not show a good scaling relation with the magnitude due to its sensitivity to the SNR. The τ_c measurements obtained from records with *Pa* smaller than 20 gal may not be sufficiently reliable because of the limited dataset. Thus, τ_c as an indicator may not be suitable for the onsite EEW using the building array system. On the other hand, *Pd* is found to be a good indicator for the destructiveness of an earthquake. All records from non-destructive earthquakes have *Pd* measurements of less than 0.5 cm, in agreement with previous results [2,4]. Furthermore, based on the analysis of the records from sensors installed at the free-field site and those at different locations inside the building, it seems that the location for the instrument does not make obvious difference in EEW practices.

Acknowledgments

This work was supported by the National Science Council (NSC) and the Central Weather Bureau (CWB) of the Republic of China. The authors wish to thank the CWB for providing strong-motion records.

References

[1] Wu YM, Kanamori H. Experiment on an onsite early warning method for the Taiwan early warning system. Bull Seismol Soc Am 2005;95:347–53.
[2] Wu YM, Kanamori H. Rapid assessment of damaging potential of earthquakes in Taiwan from the beginning of P Waves. Bull Seismol Soc Am 2005;95: 1181–1185.
[3] Wu YM, Kanamori H. Exploring the feasibility of on-site earthquake early warning using close-in records of the 2007 Noto Hanto earthquake. Earth, Planets Space 2008;60:155–60.
[4] Wu YM, Kanamori H. Development of an earthquake early warning system using real-time strong motion signals. Sensors 2008;8:1–9.
[5] Yu SB, Chen HY, Kuo LC, Lallemand SE, Tsien HH. Velocity field of GPS stations in the Taiwan area. Tectonophysics 1997;274:41–59.

[6] Wu YM, Chang CH, Zhao L, Teng TL, Nakamura M. A comprehensive relocation of earthquakes in Taiwan from 1991 to 2005. Bull Seismol Soc Am 2008;98:1471–81, doi:10.1785/0120070166.
[7] Kanamori H, Hauksson E, Heaton T. Real-time seismology and earthquake hazard mitigation. Nature 1997;390:461–4.
[8] Kanamori H. Real-Time seismology and earthquake damage mitigation. Annu Rev Earth Planet Sci 2005;33:195–214.
[9] Wu YM, Yen HY, Zhao L, Huang BS, Liang WT. Magnitude determination using initial P waves: a single-station approach. Geophys Res Lett 2006;33:L05306, doi:10.1029/2005GL025395.
[10] Wu YM, Kanamori H, Allen RM, Hauksson E. Determination of earthquake early warning parameters, τ_p and *Pd*, for southern California. Geophys J Int 2007;170:711–7.
[11] Shieh JT, Wu YM, Allen RM. A comparison of τ_c and $\tau_p^{\max}$ for magnitude estimation in earthquake early warning. Geophys Res Lett 2008;35:L20301, doi:10.1029/2008GL035611.
[12] Wu YM, Zhao L. Magnitude estimation using the first three seconds P-wave amplitude in earthquake early warning. Geophys Res Lett 2006;33:L16312, doi:10.1029/2006GL026871.
[13] Zollo A, Lancieri M, Nielsen S. Earthquake magnitude estimation from peak amplitudes of very early seismic signals on strong motion records. Geophys Res Lett 2006;33:L23312, doi:10.1029/ 2006GL027795.
[14] Wu YM, Chen YG, Chang CH, Chung LH, Teng TL, Wu FT, et al. Seismogenic structure in a tectonic suture zone: with new constraints from 2006 M_w6.1 Taitung earthquake. Geophys Res Lett 2006;33:L22305.
[15] Teng TL, Tsai YB, Lee WHK. Preface to the 1999 Chi-Chi, Taiwan, earthquake dedicated issue. Bull Seismol Soc Am 2001;91:893–4.
[16] Wu YM, Chen YG, Shin TC, Kuochen H, Hou CS, Chang CH, et al. Coseismic vs. interseismic ground deformations, faults rupture inversion and segmentation revealed by 2003 M_w 6.8 Chengkung earthquake in eastern Taiwan. Geophys Res Lett 2006;33:L02312.
[17] Allen RV. Automatic earthquake recognition and timing from single traces. Bull Seismol Soc Am 1978;68:1521–32.
[18] Shin TC. The calculation of local magnitude from the simulated Wood–Anderson seismograms of the short-period seismograms. TAO 1993;4:155–70.
[19] Wu YM, Allen RM, Wu CF. Revised ML determination for crustal earthquakes in Taiwan. Bull Seismol Soc Am 2005;95:2517–24.
[20] Yamada M, Mori J. Using τ_c to estimate magnitude for earthquake early warning and effects of near-field terms. J Geophys Res 2009;114:B05301, doi:10.1029/2008JB006080.
[21] Huang BS, Huang WG, Huang YL, Kuo LC, Chen KC, Angelier J. Complex fault rupture during the 2003 Chengkung, Taiwan earthquake sequence from dense seismic array and GPS observations. Tectonophysics 2009;466(3–4): 184–204, doi:10.1016/j.tecto.2007.11.025.